Finite Element Thermal Crack Analysis of Prestressed Double Tee Canopy Beam

Weidong Wu, Tyler K. Haraway, Asritha. S. Batchu, Ignatius Fomunung, Joseph Owino, and Mbakisya A. Onyango

Department of Civil Engineering, University of Tennessee at Chattanooga

***Abstract*: *Nonlinear Finite Element Analysis is performed to investigate the crack of a pre-stressed double tee canopy beam due to thermal expansion. Concrete damage plasticity material model is employed to detect the potential crack of concrete beam caused by thermal loads. The bond between pre-stressed strands and concrete is modeled by tie, cohesive element and friction. Explicit modeling approach is selected due to the significant discontinuity in the three-dimensional model. The potential crack pattern from FEA modeling indicates the actual crack as observed in field quite well.*

***Key words*: *Thermal expansion, Tee canopy beam, Prestress, Concrete damage plasticity, Cohesive element, Friction, Crack, Finite element, Dynamic explicit*

1. Introduction

As with much of the nation's infrastructure, the dated fleet of nuclear power plants are experiencing aging issues with many of their components, including cooling towers. Structural degradation is common with aging cooling tower components due in part to the aging mechanisms present in the near constant water environment. While structural failures of cooling tower components at nuclear power facilities typically do not lead to nuclear safety concerns, they can result in significant economic impacts due to the effect on plant operation, and the accompanying negative public perception(EPRI, 2011; Haraway, 2015).

The canopy beams are precast, pre-tensioned double tee concrete beams. Ideally these beams are simply supported, with the outside end bearing on girder beams at the inside edge of the nuclear tower cooling section. The inside end of the beams are supported by a concrete shelf poured integral with the bottom edge of the shell. Double tee beams and slabs are commonly used for roof system construction due to their structural efficiency. They are also relatively light weight when compared to other members suitable for use over long spans. Therefore, Tee Beam is well suited for forming the cooling tower canopy which generally possesses spans more than 21336mm (70 ft). As explained by Libby when discussing double tee slabs, "a significant contribution to a slab's structural efficiency results from the fact that a very large portion of the total dead load is acting on the slab at the time of prestressing (Libby, 2012)." The pre-tensioning itself acts to improve the efficiency of the member by introducing a "self-equilibrating system of internal stresses." These stresses include the tensile stress in the pretensioned tendons which in turn creates compressive stresses in the concrete (Collins & Mitchell, 1991). The result is an improved member with greater load carrying capacity than that of a normal reinforced concrete beam. In addition, double tee members are more cost effective than other types of structural members, and are widely available in most regions throughout the United States (Libby, 2012).

Unfortunately, the canopy beams investigated in this study exhibit one major degradation which have been observed and tracked during periodic preventive maintenance inspections: vertical cracking through the beam stems near the outside end of the beam as displayed in Figure 1. The issue is a concern because of the potential effect on the beams shear and flexural capacities. Additionally, the cracks provide a path for moisture to reach the embedded reinforcement leading to corrosion. The cracks observed in the beam in this study occur near the end of the beam at a location that would be well within the transfer zone where the compressive stresses being transferred from tendons to the concrete have not been fully developed. Therefore, the effect of the reinforcement stresses on crack orientation may be less prominent.

Theoretical check on strength capacity had been performed by Haraway (2015). It was found that the flexural, and shear strength capacity is not exceeded. It was discovered later that possibly the canopy beam stem crack is the result of the constraint imposed by a concrete walkway which is right on the top of the beam flanges. Both ends of the canopy beam is thus constrained and free movement at one end as expected in design is no longer guaranteed.

Finite element recently has been applied by many researchers (El-Tayeb, El-Metwally, Askar, & Yousef, 2015; Gao, Dai, Teng, & Chen, 2013; Ožbolt, Bošnjak, Periškić, & Sharma, 2014) to model the reinforced beams or frames subject to fire and elevated temperature. The thermally coupled continuum solid elements are used in those studies to capture the thermal and mechanical behavior of reinforced concrete.

When a structure is not allowed to expand, a change in temperature will lead to stress. In this work, thermal expansion due to the environmental temperature effect instead of fire is the major concern, only a thermal expansion analysis is conducted and no heat transfer is considered. Thermal expansion coefficients have been defined as part of the material properties. The interaction between strands and concrete is modeled by tie, finite thickness cohesive element and friction. Concrete damage plasticity (CDP) is defined to capture the potential crack region in the concrete double tee canopy beam.

Figure 1. Crack observed in Double Tee Canopy Beam(Haraway, 2015)

2. Materials and interface models

2.1. Concrete damage plasticity

The damage plasticity model is a continuum, plasticity-based, damage model for concrete (Abaqus User Manual). It assumes that the main two failure mechanisms are tensile cracking and compressive crushing of the concrete material under low confining pressure. In this article, concise introduction about damage indicators defined in CDP and how they are related to users provided data is given in order to help readers better understand the simulation results. Readers may refer to Hillerborg and Petersson (1976), Lubliner et al. (1989) and Lee and Fenves (1998) for details about theory of CDP.

The evolution of the failure surface is controlled by two hardening variables (plastic strains), $\tilde{\varepsilon}_t^{pl}$ and$\tilde{\varepsilon}_c^{pl}$, which are plastic strains under tension and compression, respectively. The elastic stiffness of the material is damaged (or degraded). The degradation of the elastic stiffness is characterized by two damage scalar variable variables (damage indicators), d_t and d_c $(0 \leq d \leq 1)$ which are functions of plastic strains. Zero value of d indicates no damage while "1" implies failure (Equations 1 & 2). The contour of damage variables d may be used to display potential crack pattern.

The concrete damage plasticity model assumes that the reduction of the elastic modulus is given by

$$E = (1 - d)E_0 \qquad (1)$$

and the stress

$$\sigma = (1 - d)\bar{\sigma} \qquad (2)$$

where E_0 is the initial undamaged modulus. $\bar{\sigma}$ is the effective stress tensor.

The two damage parameters d_t and d_c are functions of $\tilde{\varepsilon}_t^{pl}$, $\tilde{\varepsilon}_c^{pl}$and $\bar{\sigma}$, i.e.

$$d = d\left(\bar{\sigma}\,, \tilde{\varepsilon}^{pl}\right) \qquad (3)$$

In FEA package Abaqus, user needs to define (1) damage plasticity flow potential, yield surface and viscosity parameters (dilation angle, flow potential eccentricity, the ratio of initial equibiaxial compressive yield stress to initial uniaxial compressive yield stress, etc.); (2) compressive behavior (inelastic crushing strain $\tilde{\varepsilon}_c^{in}$ v.s. yield stress in compression σ_c, i.e. compression hardening; and inelastic crushing strain $\tilde{\varepsilon}_c^{in}$ v.s. compression damage parameter d_c, i.e. compression damage) and (3) tensile behavior (inelastic cracking strain $\tilde{\varepsilon}_t^{ck}$ v.s. yield stress in tension σ_t,i.e. tension stiffening; inelastic cracking strain $\tilde{\varepsilon}_t^{ck}$ v.s. compression damage parameter d_t, i.e. tension damage) All these parameters may be determined by four laboratory tests: uniaxial compression, uniaxial tension, biaxial and triaxial tests.

With user provided stress versus inelastic strain data, Abaqus will automatically convert to stress versus plastic-strains $\tilde{\varepsilon}_t^{pl}$ and $\tilde{\varepsilon}_c^{pl}$. Abaqus converts the cracking strain $\tilde{\varepsilon}_t^{ck}$values supplied by users in tabular to plastic strain $\tilde{\varepsilon}_c^{pl}$ using the relationship in tensile damage:

$$\tilde{\varepsilon}_t^{pl} = \tilde{\varepsilon}_t^{ck} - \frac{d_t}{1-d_t}\frac{\sigma_t}{E_0} \qquad (4)$$

where $\tilde{\varepsilon}_t^{ck}$ is the cracking strain input by user which is used to define tension stiffening and thus the strain-softening behavior for cracked concrete.

In compression damage, the relationship between the inelastic crushing strain $\tilde{\varepsilon}_c^{in}$(supplied as user input data with stress) and the plastic strain $\tilde{\varepsilon}_c^{pl}$ is:

$$\tilde{\varepsilon}_c^{pl} = \tilde{\varepsilon}_c^{in} - \frac{d_c}{1-d_c}\frac{\sigma_c}{E_0} \quad (5)$$

The material properties used in this work is shown in the Table 1 and Figures 2 and 3 (Jankowiak & Lodygowski, 2005):

Table 1. **Elastic and plastic parameters for concrete and steel**

Materials	Elastic Modulus (MPa)	Poisson's ratio	Expansion Coeff. α ($10^{-5}/^0C$)	Dilation angle	Eccentricity	f_{b0}/f_{c0}	K	Viscosity parameter
Concrete	19,700	0.19	1	38	0.1	1.12	0.666	0
Tendon	196,500	0.30	1					

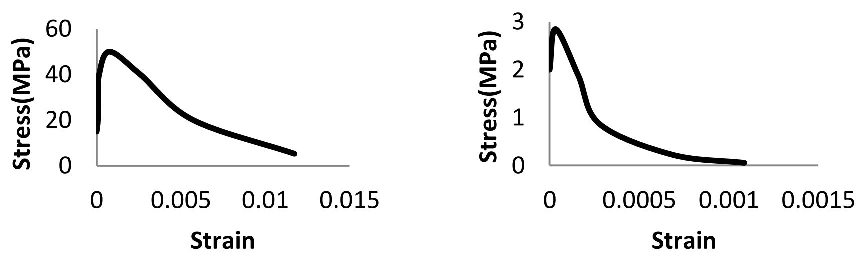

(a) (b)

Figure 2. **Concrete stress strain behavior (a) compression hardening (b) tension stiffening**

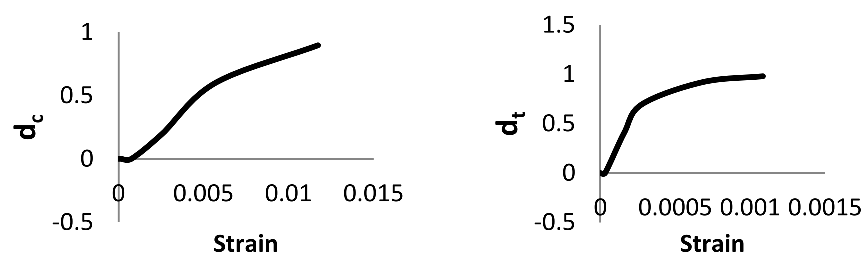

(a) (b)

Figure 3. Concrete damage parameter (a) compression (b) tension.

2.2. Concrete strands bond by cohesive elements

The interface between concrete and strands is modeled by a negligibly small thickness cohesive layer, the constitutive response of cohesive element is defined by traction versus separation (Abaqus User Manual). At initial stage, the linear elastic behavior can be described as:

$$\begin{Bmatrix} t_n \\ t_s \\ t \end{Bmatrix} = \begin{bmatrix} K_{nn} & & \\ & K_{ss} & \\ & & K_{tt} \end{bmatrix} \begin{pmatrix} \varepsilon_n \\ \varepsilon_s \\ \varepsilon_t \end{pmatrix} \qquad (6)$$

where t_n,t_s, and t_t represent the nominal tractions in the normal and the two local shear directions, respectively; while ε_n, ε_s, and ε_t denote the corresponding nominal strains. K_{nn}, K_{ss} and K_{tt} are three elastic stiffness.

Maximum nominal stress criterion is adopted to describe damage initiation and the maximum displacement with linear softening is used to determine damage evolution. The material is assumed to fail when the parameter overall damage variable D (output request SDEG in Abaqus) as given in Camanho and Dávila (2002) reaches the critical value of D_{max} (1 or 0.99) as indicated in Equation 7.

$$D = \frac{\delta_m^f(\delta_m^{max} - \delta_m^0)}{\delta_m^{max}(\delta_m^f - \delta_m^0)} \qquad (7)$$

where δ_m^{max} refers to the maximum value of the effective displacement during the loading history, δ_m^0 and δ_m^f are the effective displacements at initial of damage and at complete failure, respectively as shown in Figure 4.

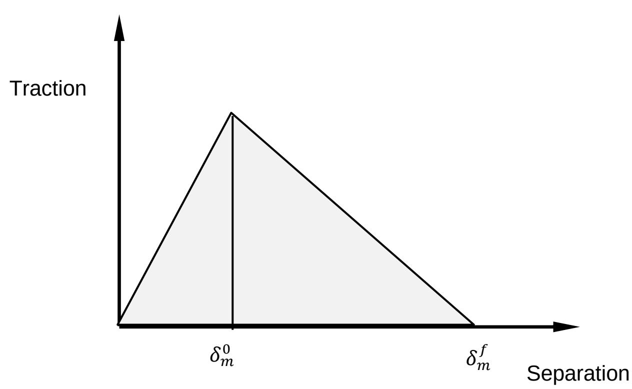

Figure 4. Linear damage evolution.

The parameters used in this work to define the cohesive bond is given in Table 2 (Yu, Jeong, Choros, & Sussmann, 2011).

Table 2. Cohesive element parameters

Materials	K_{nn} K_{ss} K_{tt} (N/mm)	Nominal stress (all three directions) (MPa)	Failure displacement (mm)
Cohesive	4,203	4.83	50.8

Surface based cohesive can be another option to model the interface, unfortunately it could not be applied in Abaqus/Explicit. A zero thickness cohesive element may be employed by construction of nodes from both rebar and concrete surfaces in a proper order, which involves writing scripts to prepare an Abaqus input file to define those zero thickness cohesive elements.

2.3. Concrete strands bond by frictional model

Another approach used in this paper to define interaction between concrete and steel strands is tie constraint (Abacus user manual) which ties concrete and strand surfaces together for the duration of the simulation. No relative movement between the two surfaces is allowed, which is analogue to a perfect bond between concrete and prestressing steel.

2.4. Concrete strands bond by frictional model

The third way to model interaction between concrete and strand is by using a friction model that defines the force resisting the relative tangential motion of the two surfaces in the mechanical contact analysis between concrete and steel. The normal behavior is defined using "hard contact" (Abaqus User Manual). A reasonable coefficient of friction 0.45 is chosen based on Baltay and Gjelsvik (Baltay & Gjelsvik, 1990; Yu & Jeong, 2015).

3. Finite element model

3.1. Geometry

The plan and cross section of the Tee beam is shown in Figure 5, length of the beam is 21,390 mm. The canopy beam is similar to the typical 8DT24 double tee beam cross section detailed in the PCI Design Handbook (Committee, 2004). They consist of two beam stems spaced 1,220 mm apart, each of which taper from 146mm at the flange to 95mm at the bottom of the stems. The beams have a total depth of 610 mm including the 50.8mm thick flange. See Figure 1 for details of the beam cross section which is based on the manufacturers drawing.

The beams are pretensioned with 5 tendons (one 9.525mm dia., and four 12.7mm dia.) in each stem. The strands follow a "harped" profile, which means they are stacked vertically being evenly spaced over the height of the stem at the ends, and depressed to the bottom of the stem in the center. In this work, we use straight strands instead in order to simplify the problem.

The continuum element used for mesh of both concrete and steel is 3D 8-node linear brick, reduced integration with hourglass control element (C3D8R). The concrete beam is discretized into 12932 elements. The mesh of the beam section is shown in Figure 5(c).

3.2. Boundaries and loadings

Both ends of the beam are constrained in horizontal direction (*Z*-direction) with simply support on the bottom, *X* symmetry (*U1*=*UR2*=*UR3*=0) is defined at one side of the flange. The tendons in the beam is prestressed at 1,303MPa (70% of the ultimate tensile strength of prestressing steel). The prestress is given as predefined field stress in initial step. Two extreme temperatures $107\ \mathrm{F}^0$ and $-10\ \mathrm{F}^0$ as recorded by National Weather Service Forecast Office are current temperatures to be defined as predefined field in load step. No external load but self-weight (gravity) is applied during simulations.

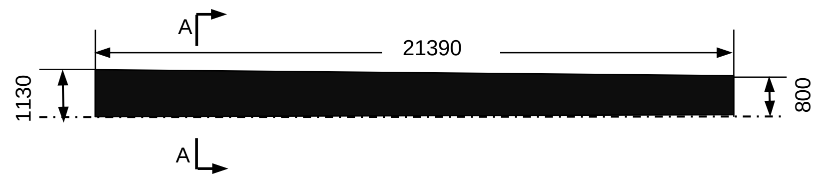

(a) Plan of the tee beam

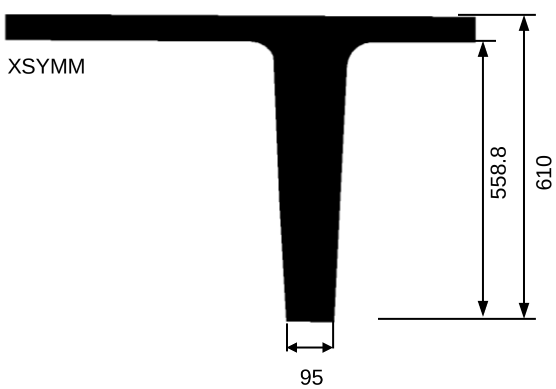

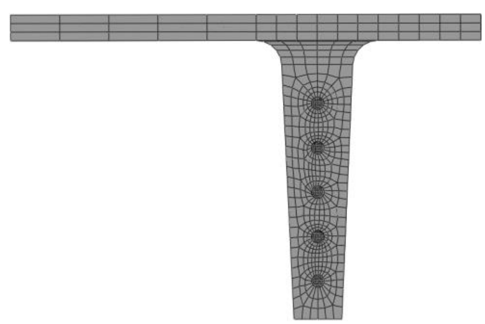

(b) Section A-A

(c) Mesh of the beam section

Figure 5. Tee beam geometry (mm).

The thermal strain is a function of the current temperature, reference temperature, and initial temperature as presented in Equation 8 (Manual)

$$\varepsilon^{th} = \alpha(\theta, f_\beta)(\theta - \theta^0) - \alpha(\theta^I, f_\beta^I)(\theta^I - \theta^0) \qquad (8)$$

where ε^{th} is thermal strain, $\alpha\left(\theta, f_\beta\right)$ is the thermal expansion coefficient, θ is the current temperature which can be created as predefined field in a certain load step. θ_0 is the reference temperature which can be specified when defining expansion coefficient as material parameter. θ_I is the initial temperature. It is assumed that no initial thermal strain exists in the tee beam, the second term in Equation 8 may be ignored.

3.3. General modeling approach

Due to the discontinuity (degradation) nature of concrete damage plasticity, crack modeling of concrete is a highly nonlinear and complex problem(Diehl, 2005), Abaqus/Explicit is selected to obtain an efficient and convergent solution(Manual). To avoid material instability due to softening in concrete damage plastic model, instability control is applied.

4. Results and conclusions

In order to study the effect of thermal expansion to the prestressed tee canopy beam, history extreme temperatures of -10F^0 and 107$\boldsymbol{F^0}$ (The National Oceanic and Atmospheric Administration) are considered in this work. The reference temperature is set to room temperature 70 F^0, no initial thermal strain is assumed.

The damage parameter d_t contour plots with variation of temperature and bond interface models are presented in Figures 6-11.

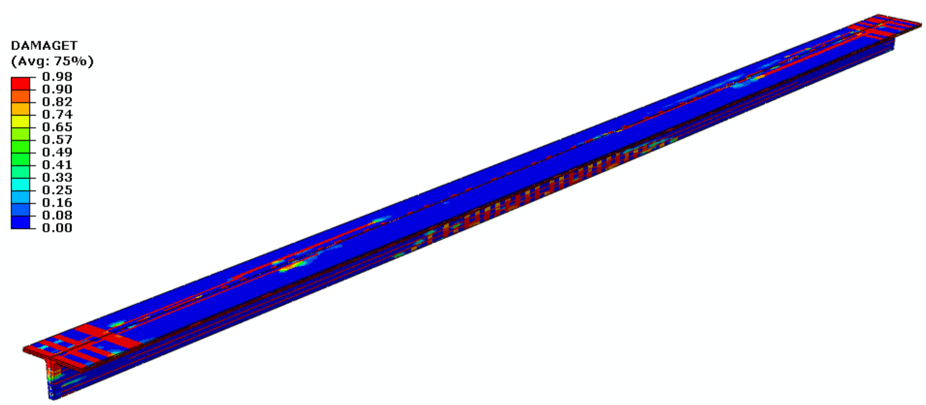

Figure 6. The damage parameter d_t when temperature is set from to 70 F^0 to 107F^0 and interface is modeled by tie

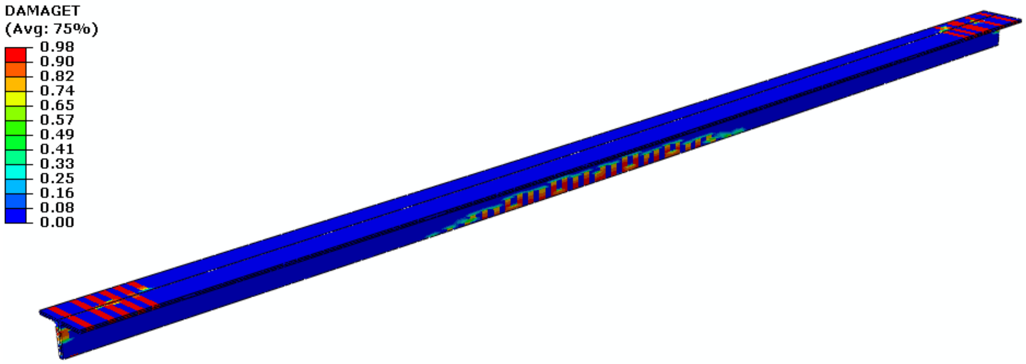

Figure 7. The damage parameter d_t when temperature is set from to 70 F^0 to -10 F^0 and interface is modeled by tie

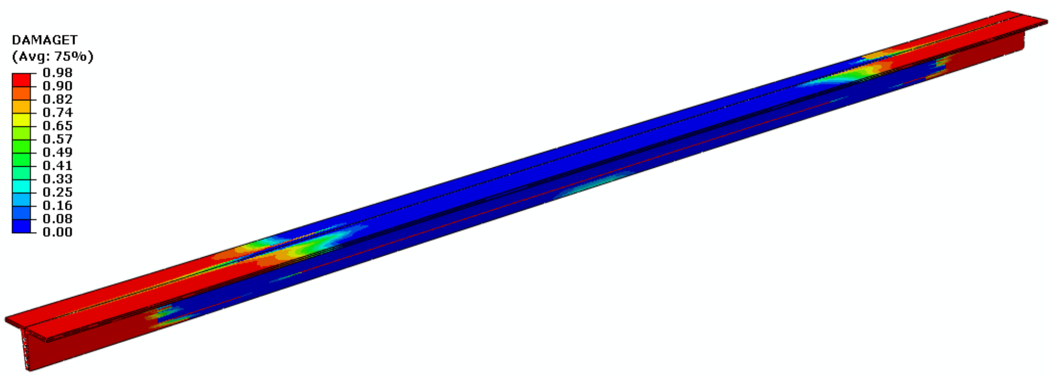

Figure 8. The damage parameter d_t when temperature is set from 70F^0 to 107F^0 and interface is modeled by cohesive elements

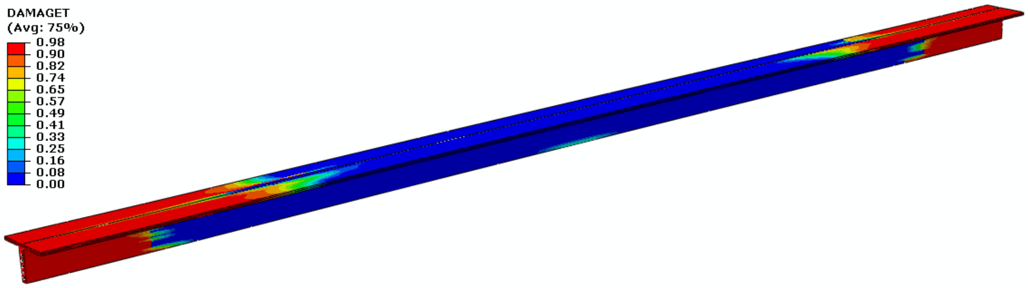

Figure 9. The damage parameter d_t when temperature is set from $70\mathrm{F}^0$ to $-10\mathrm{F}^0$ and interface modeled by cohesive elements

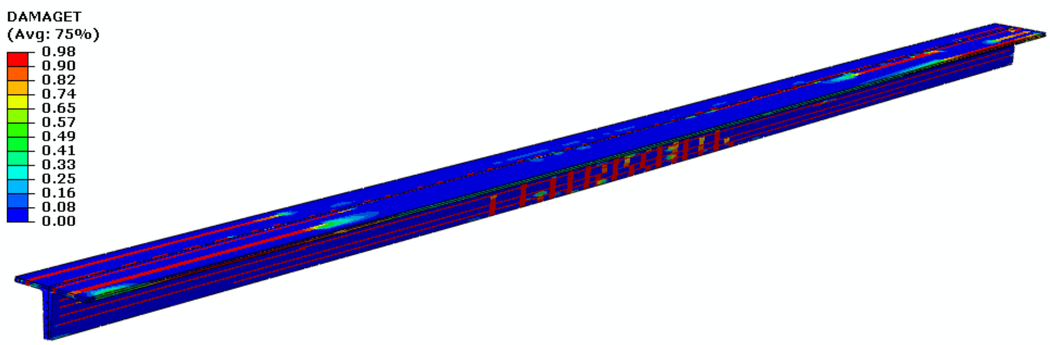

Figure 10. The damage parameter d_t when temperature is set from $70\mathrm{F}^0$ to $107\mathrm{F}^0$ and interface is modeled by friction

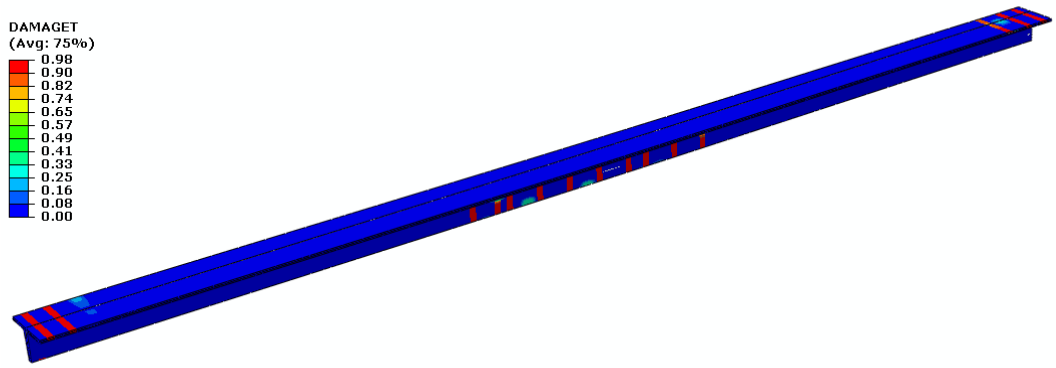

Figure 11. The damage parameter d_t when temperature is set from 70F^0 to -10F^0 and interface is modeled by friction

As indicated in the contour plots of damage parameters d_t in Figures 6-9 and Figure 11, the thermal strain due to the temperature change is relatively large at sections close to both ends especially for the case when interface is modeled by cohesive elements, which may explain why cracks were found in the beam stems near two ends. Contradictorily, the result given in Figures 10 (interface by friction, temperature changes from 70F^0 to 107F^0) show potential crack in the steel-concrete interface and the flange. A few strips in red on both ends parallel to prestressing tendons in the flange indicate potential crack. When temperature is set from 70F^0 to -10F^0 and the interface is modeled by friction, the potential crack (few strips perpendicular to the length of the beam) is found in both ends but in the flange part. Critical tension damage parameter d_t is observed in bottom of the middle section of the beam in all the simulation results. Relative smaller potential crack area in the bottom of the middle section is seen when interface is modeled by using cohesive elements.

It is noticeable that the way how to model interface between concrete and strands will have an impact on thermal expansion modeling results.

Fixed boundary conditions are defined in this work to predict the performance of the beam under thermal load. In the real structure, there may still be very limited space to allow expansion or contraction, but the actual crack found in-site is most probably caused by the thermal effect which results in large thermal strain (or stress) at both end locations.

The current models are simplified by using straight prestressing tendons. The actual prestressing steel follows a harped profile. Also, both ends of the beam are restrained. Simulation results may be improved by creating prestressing tendons following the harped profile and using more realistic boundaries.

5. References

1. Abaqus Users Manual, Version 6.14-2, Dassault Systémes Simulia Corp., Providence, RI.
2. Baltay, P., & Gjelsvik, A., "Coefficient of Friction for Steel on Concrete at high Normal Stress," Journal of Materials in Civil Engineering, vol 2, no. 1, pp. 46-49,1990.

3. Camanho, P. P., & Dávila, C. G. "Mixed-mode Decohesion Finite Elements for the Simulation of Delamination in Composite Materials,NASA/TM-2002-211737, 2002.
4. Collins, M. P., & Mitchell, D., Prestressed Concrete Structures, Prentice Hall, 1991.
5. Committee, P. I. H., PCI Design Handbook: Precast and Prestressed Concrete: MNL-120. 6th ed. Chicago, IL: PCI, 2002.
6. Diehl, T. "Modeling surface-bonded structures with ABAQUS cohesive elements: beam-type solution," Paper presented at the ABAQUS User's Conference, 2005.
7. El-Tayeb, E. H., El-Metwally, S. E., Askar, H. S., & Yousef, A. M., "Thermal analysis of Reinforced Concrete Beams and Frames," HBRC Journal, 2015.
8. EPRI.,"2011 Technical Report, Nuclear Maintenance Applications Center: Guideline for Cooling Tower Inspection and Maintenance, " pp. 280, 2011.
9. Gao, W., Dai, J.-G., Teng, J., & Chen, G., "Finite Element Modeling of Reinforced Concrete Beams Exposed to Fire," Engineering Structures, vol 52, pp. 488-501, 2013.
10. Haraway, T. K., "Analysis of Observed Degradation of Pretensioned Double Tee Canopy Beams in Hyperbolic Cooling Towers. (Master), University of Tennessee at Chattanooga, Chattanooga TN, USA, 2015.
11. Jankowiak, T., & Lodygowski, T., "Identification of Parameters of Concrete Damage Plasticity Constitutive Model," Foundations of civil and environmental engineering, vol. 6, no. 1, pp. 53-69, 2015.
12. Libby, J. R., "Modern Prestressed Concrete: Design Principles and Construction Methods," Springer Science & Business Media, 2012.
13. The National Oceanic and Atmospheric Administration, http://www.noaa.gov/weather.
14. Ožbolt, J., Bošnjak, J., Periškić, G., & Sharma, A., "3D Numerical Analysis of Reinforced Concrete Beams Exposed to Elevated Temperature, " Engineering Structures, vol. 58, pp. 166-174, 2014.
15. Yu, H., & Jeong, D., "Finite Element Bond Models for Seven-Wire Prestressing Strands in Concrete Crossties," Paper presented at the 2015 Joint Rail Conference, 2015.
16. Yu, H., Jeong, D., Choros, J., & Sussmann, T. "Finite Element Modeling of Prestressed Concrete Crossties with Ballast and Subgrade Support," Paper presented at the ASME 2011 International Design Engineering Technical Conferences and Computers and Information in Engineering Conference, 2011.

6. Acknowledgement

The first author would like to greatly appreciate Dr. Hailing Yu at Volpe National Transportation Systems Center U.S. DOT for her valuable suggestion on the interface friction model.